Modelling the behaviour of a disk of clay during pile driving using hypoplasticity

H. de Chaunac & A.E. Holeyman
Université catholique de Louvain

ABSTRACT: The bearing capacity of displacement piles in clay is usually seen to increase during the days following installation. This phenomenon is referred to as 'set-up' and occurs because during installation, the high strains imposed by the pile leave a mark on the state of the soil surrounding the pile (pore pressures, a.o.). Once installation has ended, the pore pressures generated during driving are free to dissipate, which allows the pile capacity to grow.

This paper presents a numerical simulation of a plane strain soil disk adjacent to a pile which is being driven. Emphasis is placed on the simulation of the excess pore pressure during pile penetration and afterwards, during consolidation. The soil constitutive model used is hypoplasticity for clays coupled with intergranular strain, which allows capturing the soil small strain behaviour and dilatancy. The driving analysis is performed by using a dynamic integration scheme and the consolidation is coupled.

KEYWORDS: pile driving, soil disk, numerical simulation, hypoplasticity, clay, plane strain, large strain, pore pressure.

INTRODUCTION

The driving of displacement piles brings violent distortions to the surrounding soil and, in the process, a change to the soil stress state. In consequence, as driving progresses, the effort needed to thrust the pile decreases. Once installation stops, a phenomenon referred to as 'set-up' occurs: the pile capacity grows with time. In clays, these two observations are seen to be essentially a function of the pore pressure build up and dissipation.

The experimental research done in this field peaked at the end of the last century (Soares and Dias 1989; Roy *et al.* 1981; Lehane and Jardine 1993, a.o.) and has given birth to guidelines that take into account the soil history during and after penetration (ICP-05, Jardine *et al.* 2005, Fugro-10, Van Dijk and Kolk 2010).

Nowadays, the rise of computer performance begins to allow the numerical study of the pile installation process, using Arbitrary Lagrangian-Eulerian methods (Andresen and Khoa 2013; Jassim *et al.* 2013), Coupled Eulerian-Lagrangian methods (Pucker and Grabe 2012) or hybrid methods (Basu *et al.* 2014).

In this paper, we present part of a hybrid method whose aim is to model the driving of a pile into clay: the numerical simulation of a plane strain disk of clayey soil lying around a pile (Holeyman and Legrand 1997; Figure 1) during and after a driving blow. The assumption is that during penetration and consolidation the soil can be considered as a stack of plane strain disks. The behaviour of one of these disks is investigated herein. The simulation is performed for two initial K_0 consolidated states, one normally consolidated (NC) and one overconsolidated (OC).

The paper is organised as follows. The first section offers an overview of the soil constitutive model and describes the two initial soil states considered. In the second section the numerical scheme used to model the driving blow and the consolidation is introduced. Finally, the simulation results are presented and discussed in the third section. Throughout the paper, compression is considered positive.

1 CONSTITUTIVE MODEL

The effective stress behaviour of the soil skeleton is modelled using hypoplasticity for clays (Mašín 2005) coupled with intergranular strain (Niemunis and Herle 1997). Based on the critical state theory, the hypoplastic model is three dimensional, isotropic, rate independent, and frictional with quasi-logarithmic compression. The model assumes that the soil is destructured (as defined by Leroueil *et al.* 1985), that the position of the critical state line (csl) is constant with regards to the normal compression line (ncl), that the lower limit for the void ratio is 0, and that the critical state surface is defined by the Matsuoka and Nakai (1974) surface. The intergranular strain takes into account the small strain stiffness degradation and the direction of loading, allowing the simulation of cyclic loading. One of the model strengths is that it allows for shear induced pore pressures.
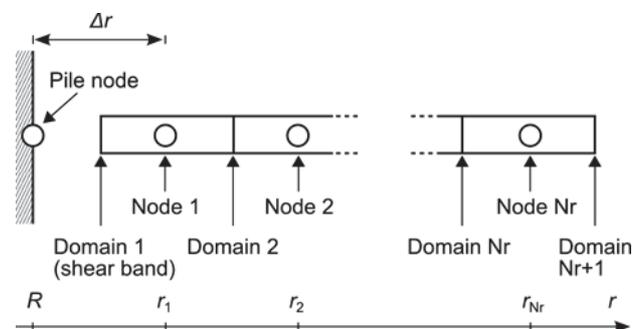

Figure 1. Spatial discretisation of the soil disk.

The soil material parameters are those of London clay, defined in Table 1, with the radial permeability taken as $k_r = 10^{-8}$ m/s. The five first material parameters are similar

to the five Cam clay material parameters while the five latter ones control the intergranular strain (see Mašín 2005 for details on the hypoplastic material parameters).

The two initial soil states chosen are defined in Table 2. These two initial states were obtained from an oedometric simulation using the hypoplastic model: first the soil was loaded to a vertical effective stress of 300 kPa, then unloaded until the overconsolidation ratio (OCR) reached 5. Starting from K_0 conditions is equivalent to saying that the pile was wished in place next to the soil disk.

Table 1. London clay hypoplastic material parameters (Mašín 2005).

ϕ'_{cs} [°]	λ^*	κ^*	N	r_M	m_R	m_T	R_M	β_r	ξ
22·56	0·11	0·016	1·375	0·4	2	2	10^{-4}	0·2	6

Table 2. Considered initial states and associated undrained shear strengths.

	OCR	σ'_{v0} [kPa]	K_0	e_0	s_{u0} [kPa]
Normally consolidated (NC)	1·1	300·00	0·68	1·14	58·5
Overconsolidated (OC)	5	11·74	3·94	1·24	38·7

It should be noted that according to the critical state theory, the position of the state with regards to the csl, i.e. the OCR, is key to the soil behaviour. In the hypoplastic model used herein, the OCR is defined as the ratio of the horizontal projection of the current mean effective stress on the isotropic normal compression line (Hvorslev's equivalent pressure p'_e) to the current mean effective stress p'_0 (Figure 2). This is not how the OCR is defined in Cam clay based models, nor is it how it is defined in geotechnical practice. Therefore, the OCR of the one dimensionally normally consolidated soil (Table 2) is higher than 1, as it would be in Cam clay but not in geotechnical practice. For the second state however, the Cam clay defined OCR would be slightly higher than 5 (depending on the slope of the unloading reloading line).

Albeit the small differences in the definition of the OCR, the quintessence of the two states defined in Table 2 is that they are each on one side of the csl (Figure 2), the first one being on the 'wet' side and the second on the 'dry' side (Schofield and Wroth 1968).
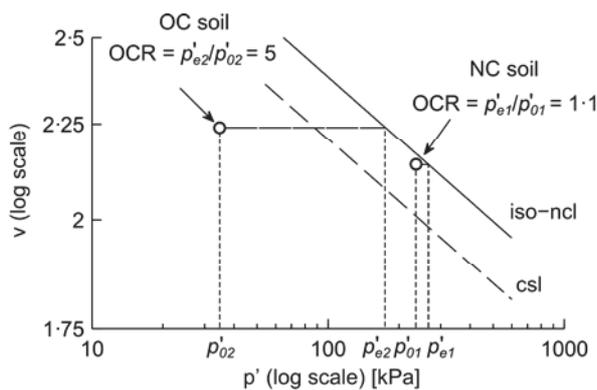

Figure 2. Considered initial states in the compression plane.

2 SOIL DISK MODEL

The soil disk is modelled using a one dimensional constant internodal distance finite difference pattern representing a layer of axisymmetric plane strain soil surrounding a pile of radius $R = 0\cdot5$ m (Figure 1). The two phases that constitute the soil are a compressible soil skeleton modelled using the aforementioned hypoplastic model and an incompressible liquid

phase. The integration scheme and boundary conditions are quite different for the driving blow and the consolidation, and are therefore detailed in the two following subsections.

2.1 Driving blow

The driving blow is assumed to happen under undrained conditions, which is imposed by making the soil skeleton incompressible.

In order to account for the finite strains, an Eulerian description is adopted wherein the kinematics of deformation are described in terms of velocity (rather than displacement) which are defined in the same way as for infinitesimal theory. This has the desirable feature that some aspects of the small strain theory are preserved (Malvern 1969).

The pile velocity is imposed at the pile node (radial position: $r = R$) and results in the displacement depicted in Figure 3, which is similar to the pile displacement observed during an *in situ* driving blow (similar amplitude, similar period, and presence of a rebound). In order to minimise wave reflections, the outer boundary, located at $r = 8R$, is an absorbing (silent) boundary (Deeks and Randolph 1994). The distance between the nodes is $\Delta r = 2$ cm.

Because of the boundary conditions, of the incompressibility and of the plane strain state, the only non trivial strain in the entire soil disk is γ_{rz}, meaning the soil disk behaves like a shear plate.

The integration scheme is performed as follows. Between each node the strain rates and effective stresses are computed, from which the vertical equation of motion is integrated to obtain vertical acceleration and velocity at the nodes. The excess pore pressures are obtained by integrating the radial equilibrium equation.

Therefore, although the constitutive model is rate independent, inertia effects of the driving blow are considered thanks to the soil disk integration scheme. In particular, the slippage between pile and soil is dependent on the pile velocity (Holeyman 1992).
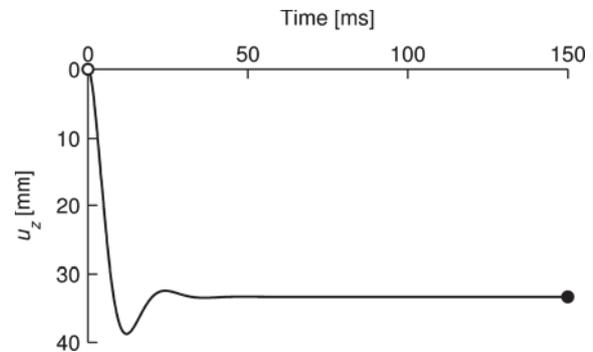

Figure 3. Vertical displacement of the pile during the driving blow.
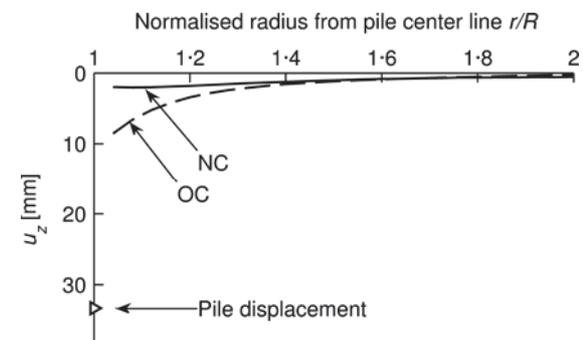

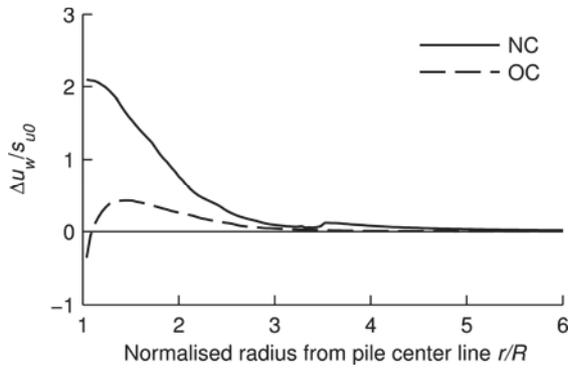Figure 4. Pile and soil vertical displacement after one blow.

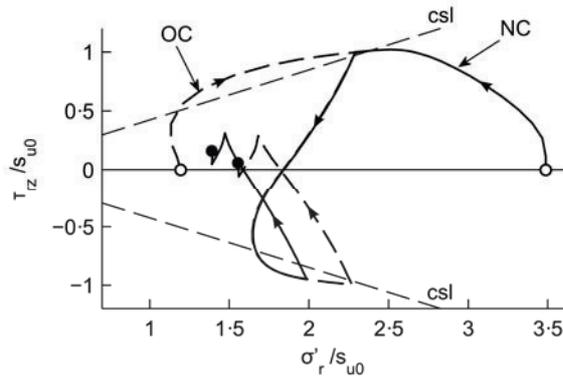Figure 5. Distribution of pore water pressure after one blow.

Figure 6. Normalised stress paths at pile-soil interface during a blow (○ and ● are respectively the initial and final states).

2.2 Consolidation

Unlike the driving blow, the consolidation analysis is assumed to happen under infinitesimal strains. The consolidation is modelled as a quasi-static coupled (pore pressure and radial displacement) process using the 'incremental' radial equilibrium (Carter *et al.* 1979). The internodal distance is $\Delta r = 8\,\text{cm}$. The pile wall is considered impermeable and the flow of water is possible only in the radial direction. The outer boundary is located at $r = 6R$. The initial conditions are those of the end of the driving blow simulation and the consolidation analysis is run for 10 000 minutes (approximately 167 hours or 7 days).

3 RESULTS

The results of the driving blow are depicted in Figure 4, Figure 5, and Figure 6.

Figure 4 shows the distribution of displacement of the pile (triangular marker) and of the soil after one blow. The pile final displacement is in excess of 3 cm but the soil, due to the high pile velocity, has yielded at a significantly smaller displacement and rests, after the blow, at a maximum displacement of 0.20 cm for the NC soil and 0.85 cm for the OC soil.

The driving blow significantly alters the stress state near the pile wall, which results in the excess pore pressure plotted on Figure 5, even though the only strain that exists is shear strain. The rebound creates a pocket of negative excess pore pressure for the OC soil but not for the NC one. As for the displacement, the effect of the blow dies out with increasing radial position.

The bump displayed by the NC soil at *3.5R* is an aftermath of the imposed changes in velocity sign of the pile: at this radius, the second positive shear wave coming from the pile has been geometrically damped just enough to a create shear strain

that implies a significant change in pore pressure, thanks to the degradation law of the soil shear modulus.

Figure 6 shows the stress path of the pile-soil interface. The OC soil reaches critical state twice (i.e. when $\tau_{rz} = \pm s_{u0}$): once in compression and once in traction. The NC soil however reaches critical state only once and therefore attains a lower final effective radial stress than the OC soil. Both soils end up on the 'dry' side of the critical state line, effectively bringing up the OCR of the NC soil but lowering it for the OC soil.

Starting from the state obtained at the end of the driving blow, the consolidation analysis is showed in the last four Figures: Figure 7 and Figure 8 for the NC soil, and Figure 9 and Figure 10 for the OC soil.

Figure 7 shows a gentle dissipation of the excess pore pressure, while the water is flowing away from the pile. At the pile-soil interface, shown in Figure 8, the effective radial stress increases as the pore pressure decreases. The total radial stress, however, decreases with the pore pressure dissipation. Also depicted on Figure 8 is the initial radial effective stress $\sigma'_{r0} = K_0 \sigma'_{v0}$.

The OC soil, with its non monotonous excess pore pressure distribution, displays a more complex history during consolidation (Figure 9) with parts of the soil undergoing both an increase and a decrease in pore pressure with time. At the pile-soil interface for instance (Figure 10) the excess pore pressure increases to a positive value and then decreases to reach the zero excess pore pressure.

The NC and OC soils respectively showed a decrease and an increase in effective radial stress during the blow (Figure 6). During consolidation, the two soils exhibit the opposite behaviour: an increase in radial effective stress for the NC soil (Figure 8) and a decrease for the OC soil (Figure 10). Nonetheless both soils, at the end of consolidation, display a lower effective radial stress than the initial one, $0.10 s_{u0}$ for the NC soil and a massive $0.53 s_{u0}$ for the OC soil.
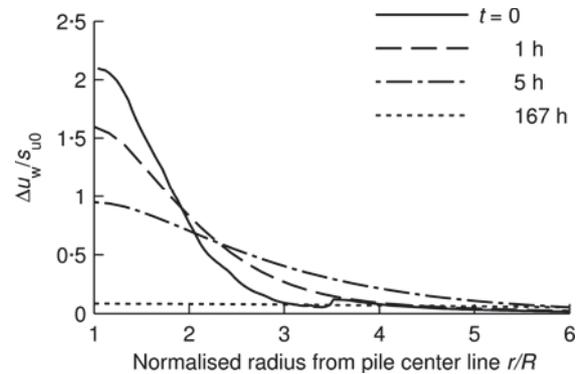

Figure 7. Pore pressure isochrones for the NC soil.
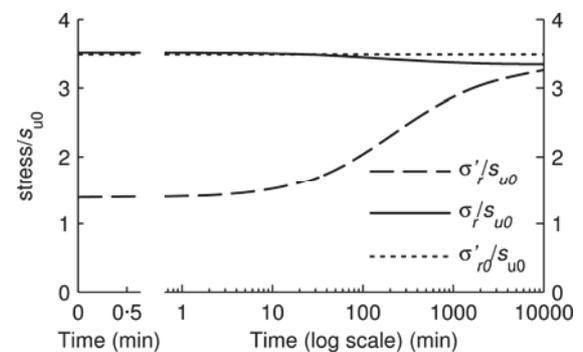

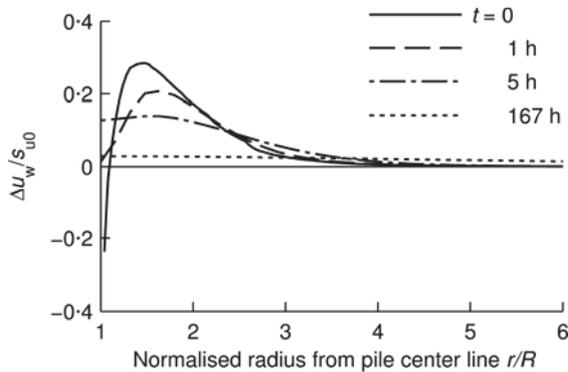Figure 8. Variation in time of radial stress at the pile-soil interface for the NC soil.

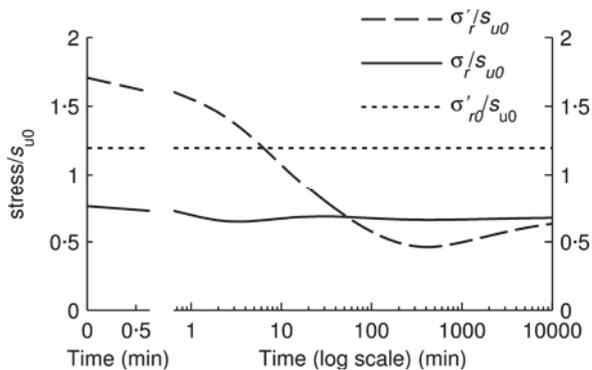Figure 9. Pore pressure isochrones for the OC soil.

Figure 10. Variation in time of radial stress at the pile-soil interface for the OC soil.

4 CONCLUSION

A numerical approach has been presented that allows the determination of stress and pore pressure changes in a saturated plane strain soil disk of clay due to a driving blow and subsequent consolidation. The soil skeleton behaviour was modelled using hypoplasticity and water was considered incompressible. Two initial states, one normally consolidated (NC) and one overconsolidated (OC), were analysed.

The overconsolidation ratio (OCR) has a significant influence on the driving blow simulation results and therefore on the stress state at the end of consolidation.

During the blow, the pile-soil interface exhibits typical behaviour corresponding to its OCR with only positive excess pore pressure for the NC soil but a pocket of negative excess pore pressure for the OC soil.

During consolidation, both soils show a decrease of total radial stress. Due to the sign of the excess pore pressure before consolidation, effective stress at the pile-soil interface rises for the NC soil but diminishes for the OC soil. Compared to their initial state, both soils end up with a lower effective radial stress at the pile-soil interface.

Finally, it should be stated that starting from a K_0 state is unrealistic because in reality the soil has already been altered by the passage of the pile toe. Therefore, a simulation taking into account the influence of the pile toe during installation is needed and is being prepared for a future publication.

5 ACKNOWLEDGEMENTS

6 REFERENCES

Andresen L. and Khoa H. D. V. 2013. LDFE analysis of installation effects for offshore anchors and foundations. *Proc. Int. Conf. Installation Effects Geotech. Eng.*, Rotterdam. Leiden, The Netherlands: CRC Press, 162–168.

Basu P., Prezzi M., Salgado R., and Chakraborty T. 2014. Shaft Resistance and Setup Factors for Piles Jacked in Clay. *J. Geotech. Geoenviron. Eng.* 140(3), 04013026.

Carter J. P., Randolph M. F., and Wroth C. P. 1979. Stress and pore pressure changes in clay during and after the expansion of a cylindrical cavity. *Int. J. Num. Anal. Meth. Geomech.* 3(4), 305–322.

Deeks A. J. and Randolph M. F. 1994. Axisymmetric time-domain transmitting boundaries. *J. Eng. Mech.* 120(1), 25–42.

Holeyman A. E. 1992. Technology of pile dynamic testing. *Proc. 4th Int. Conf. Application Stress-Wave Theory to Piles*, The Hague. Rotterdam: A. A. Balkema, 195–215.

Holeyman A. E. and Legrand C. 1997. Soil-structure interaction during pile vibratory driving. *Proc. 14th Int. Conf. Soil Mech. Found. Eng.*, Hamburg. Rotterdam: A. A. Balkema, Vol. 2, 817–822.

Jardine R., Chow F. C., Overy R. F., and Standing J. R. 2005. *ICP design methods for driven piles in sands and clays.* London: Thomas Telford.

Jassim I., Coetzee C., and Vermeer P. A. 2013. A dynamic material point method for geomechanics. *Proc. Int. Conf. Installation Effects Geotech. Eng.*, Rotterdam. Leiden, The Netherlands: CRC Press, 15–23.

Lehane B. M. and Jardine R. J. 1994. Displacement-pile behaviour in a soft marine clay. *Can. Geotech. J.* 31(2), 181–191.

Leroueil S., Tavenas F., and Locat J. 1985. Discussion: Correlations between index tests and the properties of remoulded clays by Carrier III W. D. and Beckman J. F. *Géotechnique* 35(2), 223–226.

Malvern L. E. 1969. *Introduction to the Mechanics of a Continuous Medium.* Englewood Cliffs, New Jersey: Prentice-Hall, Inc.

Mašín D. 2005. A hypoplastic constitutive model for clays. *Int. J. Numer. Anal. Methods Geomech.* 29(4), 311–336.

Matsuoka H. and Nakai T. 1974. Stress-deformation and strength characteristics of soil under three different principal stresses. *Proc. Jpn. Soc. Civ. Eng.* Vol 232, 59–70.

Niemunis A. and Herle I. 1997. Hypoplastic model for cohesionless soils with elastic strain range. *Mech. Cohes-frict. Mat.* 2(4), 279–299.

Pucker T. and Grabe J. 2012. Numerical simulation of the installation process of full displacement piles. *Comput. Geotech.* 45, 93–106.

Schofield A. and Wroth P. 1968. *Critical State Soil Mechanics.* Maidenhead, U.K: McGraw-Hill.

Soares M. M. and Dias C. R. R. 1989. Behavior of an instrumented pile in the Rio de Janeiro clay. *Proc. 12th Int. Conf. Soil Mech. Found. Eng.*, Rio de Janeiro. Rotterdam: A. A. Balkema, Vol. 1, 319–322.

Roy M., Blanchet R., Tavenas F., and La Rochelle P. 1981. Behaviour of a sensitive clay during pile driving. *Can. Geotech. J..* 18(1), 67–85.

Van Dijk B. F. J. and Kolk H. J. 2010. CPT-Based design method for axial capacity of offshore piles in clays. *Proc. 2nd Int. Symp. Frontiers Offshore Geotech.*, Perth. London: Taylor and Francis.